PHYSICAL PROPERTIES OF SAND GRAINS IN THE BAGNOLD DUNES AT GALE CRATER, MARS.

C. M. Weitz[1], R. J. Sullivan[2], M. G. A. Lapôtre[3], S. K. Rowland[4], J. A. Grant[5], M. Baker[6], and R. Aileen Yingst[1]. [1]Planetary Science Institute, 1700 E. Fort Lowell, Tucson AZ 85719 (weitz@psi.edu); [2]Cornell Center for Astrophysics and Planetary Science, Cornell University, Ithaca, NY 14853; [3]Department of Geological Sciences, Stanford University, Stanford CA, 94305; [4]Department of Geology & Geophysics, University of Hawai'i, Honolulu, HI 96822; [5]Smithsonian Institution, Washington DC, 20560; [6]Department of Earth and Planetary Sciences, Johns Hopkins University, Baltimore, MD 21218.

Introduction: The Bagnold Dunes within Gale crater on Mars consist of barchan to linear dunes and were examined along the Mars Science Laboratory (MSL) Curiosity rover traverse [1-2]. The dunes host a variety of bedforms, including meter-scale ripples with either asymmetric or symmetric profiles and smaller decimeter-scale impact ripples [3-5]. On Mars as on Earth, sand grain size and shape help constrain mobilizing wind speeds as well as transport distances along aeolian sediment pathways. Measurements of aeolian sand grain angularity and shape can help identify possible contributions from local sediment sources. For these and other reasons we used the MSL arm-mounted Mars Hand Lens Imager (MAHLI) [6] to measure grain properties at nine targets at the Bagnold dune field [7].

Four MAHLI targets were acquired during Phase 1 of the Bagnold Dunes campaign [8] (Figure 1). The target Warsaw (Sol 1182) is located a few cm below the crest of a large ripple along the edge of the stoss slope of High Dune. Targets Barby and Kibnas (Sol 1184) were just below the crest and in the trough, respectively, of a large ripple within a sand patch a few meters east of the same dune. The target Otavi (Sol 1242) was on the crest of a small impact ripple along the western margin of the barchan Namib Dune (Figure 1b).

The targets Flume Ridge (Sol 1603), Waweig (Sol 1618), Ripogenus (Sol 1638), Avery Peak (Sol 1651), and Flanders Bay (Sol 1651) were observed during Phase 2 of the Bagnold Dune campaign [2]. All except Avery Peak are downwind of a bedrock exposure between the longitudinal Nathan Bridges Dune and Mount Desert Island sand sheet (Figure 1c). Flume Ridge, Waweig, Ripogenus, and Avery Peak were along the crest of meter-scale ripples that also had oblique decimeter-scale ripples. Flanders Bay was from a surface that was disturbed by the rover wheel.

Measurements: Long axis lengths of grains were measured manually using the National Institute of Health public software package ImageJ on individual MAHLI images taken at the highest (16-23 µm/pixel) or medium (27-32 µm/pixel) resolutions, with error bars typically between 0.2-0.5 µm/pixel from the range-to-target uncertainties and ±1 pixel for our measurements. We only measured grains that were 2-3 pixels or larger [6] (the smallest measurable grain at the highest 16.2 µm/pixel resolution was ~37 µm). The population of grains 50-100 µm and finer is likely underestimated, because grain edges at these sizes were not always clearly identifiable and many were partially covered by other grains. Almost all grains measured were sand-sized, except some coarse silt grains 37-62 µm.

Circularity (4πArea/Perimeter^2) and aspect ratio (major axis length/minor axis length) of 100 grains larger than 150 µm from each target except Kibnas and Waweig were calculated from shapes outlined in ImageJ (measuring grains >150 µm ensured >10 vertex points spaced 10-20 µm apart to define the shape of each grain). Grain shape could not be measured at Kibnas and Waweig due to lower resolution images and the predominance of grains <150 µm. Circularity and aspect ratio are analogous to the sphericity index commonly used to define grain shape (where 1.0 indicates a perfect circle), and influence grain transport and deposition.

Results from Phase 1: Measurements of the Barby and Warsaw targets indicate a unimodal grain-size distribution between 100-750 µm, with a ~350 µm median at both targets. Small (30-50 µm size) dust aggregates are present at Warsaw, suggesting sands there were not active as recently as those at Barby. The Kibnas ripple trough appears to be more representative of finer grains (50-150 µm, median 117 µm) that dominate most of the High Dune stoss surface, based on relating MAHLI images to Mastcam images covering large portions of the dune. The grains at Kibnas were too small to permit shape measurements.

The MAHLI image of Otavi displayed 50-350 µm grains, with most between 100-150 µm and a median of 127 µm, consistent with previous measurements [4,9]. The grains appear slightly less circular and more elongate at Otavi than at either Barby or Warsaw.

Compositional data indicate depletion of volatiles and enrichment in mafic minerals in the Bagnold sands relative to other soils at Gale crater [10-15], presumably due to the lack of dust and sorting within the active dune sands. Segregation of grain size between crests and troughs also influences the composition, with the Barby crest being richer in feldspar and the Kibnas trough having more olivine and pyroxene [13].

Results from Phase 2: For Phase 2 of the Bagnold Dunes campaign, grain sizes varied from 37-575 µm for Ripogenus, which was the least sorted among the five targets analyzed in the southern part of the dune field (Flume Ridge, Waweig, Ripogenus, Avery Peak, and Flanders Bay). All five of these targets have medians between 110-132 µm, similar to Otavi and Kibnas. Mastcam false color images across the low-relief Nathan Bridges Dune and Mount Desert Island sand sheet show possible compositional sorting of grains across large ripples, with generally bluer stoss slopes and crests compared to the redder lee slopes. The Flanders Bay image was acquired over disturbed sand within a rover wheel track, so it represents a mixture of surface and subsurface materials.

Grains at Flume Ridge have the most elongate shapes of all the active sand targets, with a median aspect ratio of 1.25. MAHLI stereo images here obtained ~3 minutes apart showed individual sand grains moving a few hundred micrometers. Sand movement was evident also in other rover camera images, with transport to the WSW [16]. APXS compositional data support low dust (i.e., low S, Cl, and Zn) due to high wind activity at the linear dunes [14].

Conclusions: The median size range of active sand at the Bagnold Dunes is narrow and the majority of sizes are very fine (50-150 µm), except at the base of the stoss surface of High Dune, consistent with expectations there of coarser grains collecting along the dune's trailing edge [e.g., 4]. We do not believe that differences in particle size distributions between Bagnold Phases 1 and 2 locations were affected by differences in wind activity (Bagnold Phase 1 data were acquired during inactive winds, unlike Phase 2 data). Instead, grain size differences between Phase 1 and 2 appear to reflect target location within the dune field and their local positions on bedforms of different sizes and morphologies.

Friction speeds derived from atmospheric modeling almost never reach fluid thresholds expected to mobilize 110-132 µm grain sizes measured on the ripples [17]. Instead, aeolian surface creep of coarser grains (>300 µm) caused by impacts from finer saltating grains may explain coarser grain movement under current martian wind speeds. Additionally, grains mobilized at low wind speeds between the impact and fluid thresholds can splash other grains, resulting in the gradual movement of bedforms over time [9].

References: [1] Chojnacki M.. and Fenton L.K. (2017) *J. Geoph. Res. Planets, 122*, 2216-2222; [2] Lapôtre M.G.A. and Rampe E.B. (2018) *Geophys. Res. Letts. 45*, 10200-10210; [3] Lapôtre M. et al. (2016) *Science 353*, 55-58; [4] Ewing R. et al., (2017) *J. Geoph. Res. Planets, 122,* 2544–2573; [5] Lapôtre M. et al. (2018) *Geophys. Res. Letts. 45*, 10,229-10,239. [6] Edgett K.S. et al. (2012) *Space Sci. Rev. 170*, 259-317. [7] Weitz C.M. et al. (2018) *Geophys. Res. Letts 45*, 9471-9479; [8] Bridges N. and Ehlmann B. (2017) *J. Geophys. Res. Planets, 122*, doi:10.1002/2017JE005401. [9] Sullivan R. and Kok J. (2017) *J. Geoph. Res. Planets*, *122*, 2111– 2143. [10] Achilles C. et al. (2017) *J. Geoph. Res. Planets, 122*(11), 2344-2361; [11] Cousin A. et al. (2017) *J. Geophys. Res. Planets, 122*, 2144–2162; [12] Ehlmann B. et al., (2017) *J. Geophys. Res. Planets*, doi: 10.1002/2017JE005267; [13] O'Connell-Cooper C. et al. (2017) *J. Geophys. Res. Planets*, *122*, 2623– 2643; [14] O'Connell-Cooper C.D. et al. (2018) *Geophys. Res. Letts. 45*, 9460-9470; [15] Rampe E.B. et al. (2018) *Geophys. Res. Letts. 45*, 9488-9497; [16] Baker M. et al. (2018)) *Geophys. Res. Letts. 45.* 8853-8863. [17] Baker M. et al. (2018) *J. Geoph. Research*, *123*, 1380-1394. [2018].

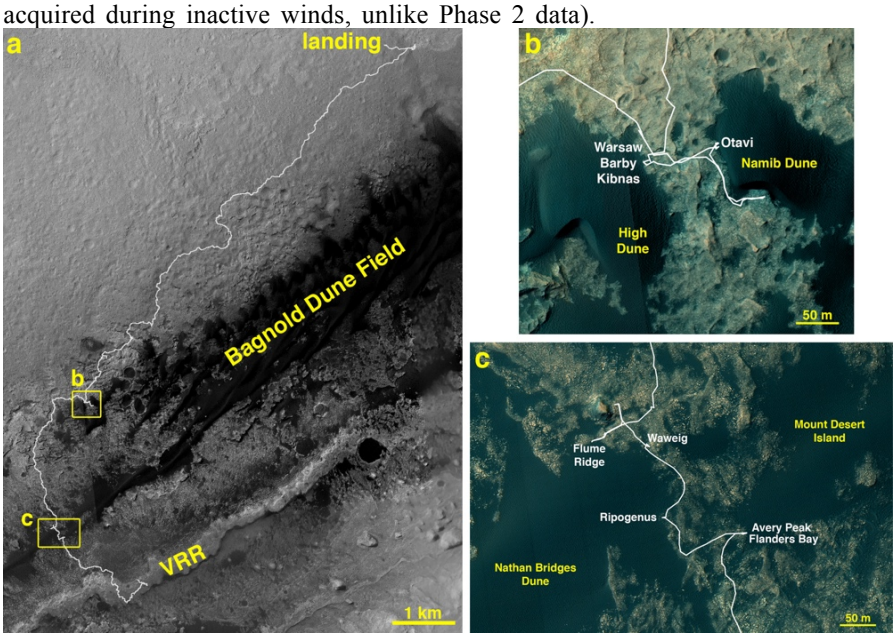

Figure 1. (a) HiRISE mosaic showing the Curiosity rover traverse from the landing site in the upper right to Sol 2038 position on the Vera Rubin Ridge (VRR). Yellow rectangles outline locations of panels b and c. (b) The four targets of Phase 1. (c) The five targets of Phase 2.